Sparse Broadband Acoustic Response Estimation via a Gaussian Mixture Model with Application to M-ary Orthogonal Signaling

Paul J. Gendron
Maritime Surveillance Division, Code 56490
Space and Naval Warfare Systems Center Pacific, San Diego CA, USA.
paul.gendron@navy.mil

ABSTRACT

Shallow water acoustic response functions at high frequencies and large bandwidths exhibit spatio-temporal variability that depends greatly on the propagation media's volume and boundary conditions as well as system source-receiver motion. For this reason practical acoustic systems invariably must operate without perfect knowledge of the space-time state of the ocean media. Considered here is a Gaussian mixture assignment over Doppler and channel bandwidth employed to describe the amplitude and phase of such acoustic response functions over signal duration and bandwidth that can serve in many scenarios to replace recursive least squares and Kalman-like algorithms. The mixtue Gaussian model of channel dynamics allows for the accurate and adaptive description of the response function. The model is flexible and naturally accommodates varying degrees of observed channel sparsity. Posterior expectations are derived and shown to be soft shrinkage operators over Doppler-channel frequency. The model allows for novel and accurate estimates regarding the aggregate acoustic path dilation process that serve to replace conventional phase locked loops. This adaptive filtering scheme with aggregate path dilation estimation and compensation is tested on M-ary orthogonal signals at both 1 and 2 bits per symbol during the Unet08 acoustic communication experiments. These tests took place in the downward refracting, lossy bottom environment of St. Margaret's Bay Nova Scotia off of the R/V Quest. Receiver algorithms based on this approach were applied to a single element acoustic time series and empirical bit error rates demonstrate a 4 dB improvement over rank based maximal path combining methods. For a single hydrophone at 2 bits per symbol a bit error rate of less than 10^{-4} is observed at received SNR < -10 dB corresponding to an SNR/bit < 14 dB.

1 INTRODUCTION

This work is concerned with the basic problem of accurately estimating the time varying broadband acoustic Green's function in dynamic shallow water environments from observed measurements at very low signal to noise ratios (SNRs). The methods are fundamentally adaptive filtering schemes and constitute an essential component to a wide range of signal analysis methods from medical diagnostics [16] and classification of volume density from ultrasound backscatter [8] to acoustic communications applications [11][18] . Conventional approaches in the context of acoustic communications include variants of least mean square, recursive least squares and the Kalman filtering algorithm[2][10][15]. These approaches fundamentally leverage the temporal coherence of the Green's function through appropriate averaging to ensure that the resulting estimates are statistically efficient. One shortcoming of these algorithms is that they are typically employed in a look-back framework, only exploiting preceeding observations to make inferences regarding the present time sample. By marching forward in time and leveraging a Markov assumption regarding the process, these algorithms exploit a temporal model of the dynamics of the response process to make an estimate of the present state. For the case of observations over a finite duration window, more data can be brought to bear on the estimation problem and greater statistical efficiency can be attained. The time-recursive Gauss-Markov framework is capable of being adapted to such scenarios by employing forward-backward methodologies to fully exploit the temporal dependencies.

This article develops and demonstrates an estimation scheme based on a mixture-Gaussian model over time/Doppler and frequency/selectivity such that the Green's function at any instant can be estimated given all of the data over the entire duration and bandwith of the signal[9]. The resulting mixture-Gaussian framework allows for a level of flexibility in the regularization that is not as easily accomplished with Gauss-Markov models short of full forward-backward recursions. The latent parameters of the mixture model succinctly and parsimoniously capture the degree of sparsity encountered in underwater acoustic environments. Presented here is a modeling framework for time varying acoustic response functions that can serve the practical needs of acoustic parameter estimation as well as coherent underwater acoustic communications. Much like forward-backward recursions the proposed adaptive filtering method allows for the efficient use of all of the observations within the signaling epoch to make inferences regarding each time instant within that epoch.

1.1 Joint channel and symbol estimation

The specific application to be explored here is that of adaptive filtering applied to underwater acoustic communication receivers where estimates of the acoustic response enable coherent multipath combining. Let the measurements at the acoustic receiver be represented by $\mathbf{r}$, the acoustic response over the broadband channel as $\mathbf{h}$ and let $\mathbf{b}$ represent the symbols sent. An acoustic communication receiver can be broadly described as a set of symbol decision rules $\hat{\mathbf{b}} = D_{\mathbf{h}}[\mathbf{b}|\mathbf{r}]$ that extract the relevant information regarding the symbols from the received data. However since the prior constraints on the acoustic response function are not easily analytically averaged out over the conditional density of the data the optimal solution

$$\begin{aligned} \hat{\mathbf{b}} &= \arg\max_{\mathbf{b}} \int p(\mathbf{r}|\mathbf{h},\mathbf{b}) \times p(\mathbf{h})\ d\mathbf{h} \\ &= \arg\max_{\mathbf{b}}\ E_{\mathbf{h}}\ [p(\mathbf{r}|\mathbf{h},\mathbf{b})] \end{aligned} \quad (1)$$

can be unwieldy. While the conditional model of the received data $p(\mathbf{r}|\mathbf{h},\mathbf{b})$ will almost invariably be a multivariate Gaussian density and the bit coding scheme allows $p(\mathbf{b}|\mathbf{h},\mathbf{r})$ to be well specified [15] the marginal $p(\mathbf{b}|\mathbf{r})$ is an average over an acoustic channel of high dimension residing in a much higher dimensional (>1000) delay-Doppler space. This makes computing $\hat{\mathbf{b}}$ a significant challenge. For this reason it is useful to break up the problem into a few simpler ones that are more easily handled and for which tractable and computationally less burdensome solutions can be derived. The solution $\hat{\mathbf{b}}$ can be well approximated by solving a sequence of conditional optimization problems in the parameters of $\mathbf{h}$. The result is a set of estimators for the channel parameters and a set of decision rules conditioned on those channel estimates.

$$\begin{aligned} \hat{\mathbf{h}}^i &= E_{h|b=\hat{b}}[\mathbf{h}|\mathbf{r},\mathbf{b}=\hat{\mathbf{b}}^{i-1}] \\ \hat{\mathbf{b}}^i &= \arg\max_{\mathbf{b}} p(\mathbf{b}|\mathbf{r},\mathbf{h}=\hat{\mathbf{h}}^i)\ . \end{aligned} \quad (2)$$

This sequence characterizes the channel estimation based receiver approach taken here. Various optimization schemes for each conditional density may be chosen and associated algorithms follow. More accurate rules can be derived, for instance the channel conditional expectation based on the symbol decision could rather be weighted over symbol probabilities,

$$\hat{\mathbf{h}}^i = E_{b|r}E[\mathbf{h}|\mathbf{r},\mathbf{b}]$$

rather than simply conditioned on the argmax: $\hat{\mathbf{b}}^i$. Use of such $soft$ decision rules would lead to weighted averages with added computational costs but no greater conceptual hurdle. The receiver structure takes advantage of the analytic simplicity of the conditional densities of the channel and symbol parameters to approximate the maximizing argument of the marginal density. Adaptive filtering, the estimation of the channel state, is therefore critical for coherent multipath combining in time varying environments.

1.2 Organization of this article

The remaining sections of this article are organized as follows: Section 2 presents the salient features of shallow water acoustic response functions and associates the dynamic parameters with the delay-Doppler acoustic response. Section 2 then goes on to present the Gaussian mixture model as a means of describing the sparse delay-Doppler arrivals of acoustic response functions. The section goes on to derive estimators for the acoustic response function given a received time series. Section 3 presents an aggregate path dilation process model and shows how accurate estimates of the acoustic response function can be used to unravel bulk correlated path delay time processes. Section 4 presents various acoustic communication receiver algorithms for M-ary orthogonal signaling based on the proposed adaptive filtering scheme. Section 5 presents results from an M-ary orthogonal signaling experiment taken during at-sea tests in St. Margaret's Bay. Section 6 presents summarizing statements, conclusions and future work.

2 MODEL OF UNDERWATER ACOUSTIC RESPONSE

Each acoustic path linking source and receiver exhibits geometric spreading and frequency dependent volume attenuation [12][20]. Let $l_{m,t}$ represent the acoustic path length of the m^{th} acoustic path at time t and let $\tau_{m,t} = \int_{l_{m,t}} d\mathbf{s}/c(s,t)$ represent its propagation delay. The amplitude and phase contribution of the pressure field at the receiver due to the m^{th} path is

$$\begin{aligned} h_{m,t,f} &= l_{m,t}^{-1+\epsilon_m} \times e^{-\alpha(\omega)l_{m,t}+\sum_k \gamma_{m,k}(\omega)} \times e^{-j\omega\tau_{m,t}} \\ &= a_m(t,f) \times e^{-j\omega\tau_{m,t}} \qquad \omega = 2\pi f. \end{aligned} \quad (3)$$

The first term captures attenuation due to geometric spreading and with $|\epsilon_m| << 1$ the refractive effects through the volume. The second term summarizes the volume attenuation due to sea-water absorption losses [12][20]. The term $\sum_k \gamma_{m,k}(\omega)$ summarizes the boundary interactions where Re$\{\gamma\}$[nepers], Im$\{\gamma\}$[radians]. Here $\gamma_{m,k}$ is the reflection coefficent of the k^{th} boundary interaction along the m^{th} acoustic path. The final term captures the aggregate phase rotation associated with propagation over the acoustic path. The phase rotation is a linear funtion of frequency as the sound speed and thus $\tau_{m,t}$ is not a function of frequency. The aggregate acoustic response function is the superposition of these M_{path} acoustic contributions

$$h_{t,f} = \sum_{m}^{M_{path}} h_{m,t,f}. \quad (4)$$

The inverse Fourier transform of Eq. (4) is the response function over path-delay and geo-time and can be expressed as

$$\begin{aligned} h_{t,\tau} &= \textstyle\sum_m^{M_{path}} \psi_{m,t}(\tau-\tau_{m,t}) \\ \psi_{m,t}(\tau) &= (2\pi)^{-1}\int a_m(t,\omega/2\pi) \times e^{j\omega\tau}\ \ d\omega. \end{aligned} \quad (5)$$

Here notation is simplified by retaining h as the response function regardless of the basis functions or domain over which it is defined. The response function can likewise be represented over the delay-Doppler domain with

$$\begin{array}{l} h_{\Delta,\tau} = \sum_{m}^{M_{path}} \psi_{m,\Delta}(\tau) \\ \psi_{m,\Delta}(\tau) = \int_{I_T} \psi_{m,t}(\tau - \tau_{m,t}) e^{-j\Delta t} dt. \end{array} \quad (6)$$

The total delay spread of the multi-path channel is

$$\tau_{max} = \max_{m,t}\{\tau_{m,t}\} - \min_{m,t}\{\tau_{m,t}\}. \quad (7)$$

Underwater acoustic response functions can vary greatly across ocean environments as well as over time in a given ocean environment. Certain bottom materials and roughness, water sound speed and surface wave spectra imply certain acoustic response functions and these can vary greatly spatially and temporally. Given the environmental conditions numerical solutions to acoustic propagtion can be useful in revealing the characteristics of broadband acoustic channel conditions [12] however acoustic receiver algorithms must be robust to spatial and temporally varying channel conditions with limited or no prior information regarding any of the acoustic environment parameters. The algorithms must effectively construct the essential parameters of the response from the measured pressure field. Because of the unknown and diverse range of channel conditions a significant hurdle in underwater acoustic receiver algorithms is that the underlying model must not place severe restrictions on the temporal or spatial variations of the functions $\{\psi_m, \tau_m\}_{m \leq M_{path}}$ between communication epochs while simultaneously parsimoniously allowing for their variation within a signaling epoch. Such parsimonious representation allows for the low variance estimation of the response function while giving flexibility to handle quite different environments.

In the approach presented here two features of shallow water acoustic response function are exploited. First, their sparsity, the interarrival durations on average exceed the delay bandwidth of the intra-path spreading functions $\psi_m(\tau)$. Explicitly, with $\hat{\psi}_m(\tau) = \psi_m(\tau)/\sum \psi_m(\tau)$ it is postulated that $E[\sqrt{\int \tau^2 \hat{\psi}_m(\tau) d\tau}] < E[|\tau_m - \tau_n|])$ where the expectation operator $E[\cdot]$ is over the observed sample space of environments. Secondly it is postulated that the arrival delay processes $\tau_m(t)$ of the various paths for a given signaling epoch exhibit significant temporal correlation. This assumption is attributed to the fact that angle spreads of propagating paths in ocean waveguides are very small, typically less than 20^o often less than 5^o so that the dominant motion within the horizontal plane couples similarly to all coherent delay paths.

2.1 Model of passband frequency translated underwater acoustic response

Using the passband basis functions $\{e^{j\omega_c t}\phi(t - n/W)\}_{n \in I}$ of bandwidth W, centered at time n/W and frequency $f_c = \omega_c/2\pi$, express the M-ary orthogonal spread spectrum communication signal as

$$s_t = e^{j\omega_c t} \sum_n c_n^{\mathbf{b}} \phi(t - n/W). \quad (8)$$

Here the notation $c_n^{\mathbf{b}} = c_{<n>_{N_s}}^{b_{\lfloor n/N_s \rfloor}}$ is employed allowing the sent signal to be unencumbered with the specification of the duration N_s of the signaling frame. At the receiver the signal is

$$Hs(t) = \int h_{t,\tau} s_{t-\tau} d\tau$$

and with the simplified broadband channel model (4) express this time-frequency distorted signal as

$$\begin{array}{r} Hs(t) \times e^{-j\omega_c t} = \sum_{m,n} c_n^{\mathbf{b}} e^{-j\omega_c \tau_{m,t}} \int \psi_{m,t}(\tau - \tau_{m,t}) \\ \times e^{-j\omega_c(\tau - \tau_{m,t})} \phi(t - \tau - n/W) d\tau. \end{array} \quad (9)$$

Expressing the baseband translated and filtered acoustic response function for the m^{th} path as

$$\tilde{\psi}_{m,t}(\tau) = \int \psi_{m,t}(\tau') \times e^{-j\omega_c \tau'} \phi(\tau - \tau') d\tau'$$

results in

$$Hs(t) \times e^{-j\omega_c t} = \sum_n c_n^{\mathbf{b}} \times h_{t,t-n/W} \quad (10)$$

$$h_{t,\tau} = \sum_m e^{-j\omega_c \tau_{m,t}} \tilde{\psi}_{m,t}(\tau - \tau_{m,t}).$$

The key features of the acoustic response (11) are now identified. First, time variations in the acoustic path delays $\tau_{m,t}$ imply both time varying phase modulations ($e^{j\omega_c \tau_{m,t}}$) and time varying arrival times of the phase-fronts ($\tau_{m,t}$). As previously mentioned the phase fronts are not dispersed since sound speed is not a function of frequency. Most of the energy is captured in a small set of delay times and therefore acoustic response functions are generally sparse with dominant arrivals occupying a relatively small proportion of the τ_{max} duration delay band. Secondly since angle spreads are small in the horizontal ocean waveguide the temporal process of the delay times exhibit considerable correlation.

The linear model (10) can be expressed as a sampled discrete time $t = \rho \times n'/W$ version as

$$Hs(n') \times e^{-j\rho\omega_c n'/W} = C_{\mathbf{b}}\mathbf{h} \ . \quad (11)$$

and letting $I_T = \{0 < t < T\}$ be the $K \times N_s/W + \tau_{max}$ duration communication packet interval and $I_\tau = [\max\tau_m(t), \min\tau_m(t)]$ the passband translated acoustic response function can be represented in the delay-Doppler domain as,

$$h_{\Delta,\tau} = \sum_m \int_{I_T} e^{-j2\pi\Delta t - j\omega_c \tau_{m,t}} \times \tilde{\psi}_{m,t}(\tau - \tau_{m,t}) dt$$

which is simply expressed as,

$$h_{\Delta,\tau} = U_\Delta h_{t,\tau} \quad (12)$$

where U_Δ is the Fourier transform from geo-time to Doppler frequency. The channel response function can likewise be represented in the Doppler[Hz]-selectivity/frequency[Hz] domain via

$$h_{\Delta,f} = \int_{I_\tau} e^{-j2\pi f\tau} h_{\Delta,\tau} \quad d\tau$$
$$\Leftrightarrow \quad h_{\Delta,f} = U_{\Delta,f} h_{t,\tau} \tag{13}$$

where $U_{\Delta,f}$ is the 2-D Fourier transform from geo-time[sec] and delay[sec] to Doppler[Hz] and selectivity[Hz]. Likewise the passband filtered and baseband translated acoustic response function can be represented in the time-frequency domain as

$$h_{t,f} = \sum_m \phi(f) a_m(t, f + f_c) e^{-j2\pi(f+f_c)\tau_{m,t}}$$
$$\Leftrightarrow \quad h_{t,f} = U_{t,f} h_{t,\tau} \tag{14}$$

where it is understood that the argument denotes the Fourier transform, $\phi(f) = \int \phi(t) e^{-j2\pi f t} dt$.

2.2 Prior density for acoustic response function

Underwater acoustic response functions can vary considerably as a function of the environment. In order to capture this prior variability or uncertainty in the acoustic response function in such a way that variations are modeled in a parsimonious and yet flexible and accommodating way consider the use of an adaptive scheme suited for sparse time-varying channels. The notion of sparsity simply captures the fact that typical acoustic response functions obey the rule: $M_{path} < W\tau_{max}$. It is useful to view each delay-Doppler slot therefore as a possible ensonified acoustic path between source and receiver. Each of these slots will have a prior probability of being acoustically occupied, coherently linking source and receiver. Acoustic path occupation likelihood at a given delay-Doppler is set by a probability $\pi_{\Delta,\tau}$ that is a function of the Doppler frequency. The amplitude and phase of the occupied Doppler-frequency slot will be hypothesized as Gaussian with zero mean and a known variance. For the unoccupied slots it is also postulated that the amplitude and phase are Gaussian however the unoccupied slots are naturally associated with a much smaller variance. The probability density function of the channel's amplitude and phase at any given slot is therefore modeled by a binary mixture Gaussian model that is fully specfified by two variances and a probability that the slot is in one of the given states. These prior assumptions are captured in the following hierarchical Bayesian model,

$$h_{l,k}|z_{l,k} \sim N_{h_{l,k}}^{z_{l,k}}(0, \lambda_k^2) \times N_{h_{l,k}}^{1-z_{l,k}}(0, \epsilon_k^2) \tag{15}$$

$$z_{\Delta,\tau} \sim Ber(\pi_{\Delta,\tau}), \quad \pi_{\Delta,\tau} = \pi_0 D(\Delta) \times U_{0,\tau_{max}}(\tau)$$
$$\int_I D(\Delta) d\Delta = 1.$$

The factor π_0 is the a priori sparsity. The factor $D(\Delta)$ is a marginal or average Doppler spectrum and captures the prior likelihood of the ensonified channel paths' scatterers possessing a given aggregate velocity $v = c_{speed} \times \Delta / f_c$. This average Doppler spectrum has the interpretation of a probability density function. Given τ_{max} the delay profile U is a uniform density. Regarding Doppler spread, two physical processes are worth considering. First there is the Doppler offset associated with initialization and estimation of source and receiver clock rate offsets and relative platform speeds. This spread can be quite large and will depend on both the time-bandwidth product of the initializing synchronization waveform and the acceleration rate of the platforms. The second is the inherent Doppler spread associated with the acoustic response function and captures for instance the different path dilation rates. It is accepted that actual acoustic path amplitudes and phases with their times of arrival known do not necessarily obey a Gaussian density. While propagation modeling over actual underwater environments and geometries could provide insight into the actual densities of the channel coefficients it would require environmental information that is not availale to most underwater systems. The proposed model is useful because it allows for the parsimonious treatment of sparse time varying arrivals and the analytic solution of all posterior moments leading to computationally reasonable solutions. The mixture weights π and spectrum $\bar{\lambda}, \bar{\epsilon}$ could likewise be tuned with dependencies across delay-Doppler. For now it is accepted that the model, while not proved from propagation physics, offers an inductive framework that captures the essential spectral features of shallow water acoustic response functions. It thereby provides a useful adaptive structure for estimation of the response from observations.

It is also useful to consider a similar Gaussian mixture model on the Doppler-selectivity domain

$$h_{l,k}|z_{l,k} \sim N_{h_{l,k}}^{z_{l,k}}(0, \lambda_k^2) \times N_{h_{l,k}}^{1-z_{l,k}}(0, \epsilon^2)$$

$$z_{\Delta,f} \sim Ber(\pi_{\Delta,f}), \quad \pi_{\Delta,f} = \pi_0 D(\Delta) \times S(f). \tag{16}$$

The parameters π, $\bar{\lambda}$, and $\bar{\epsilon}$ can be estimated from the data as in [9].

2.3 Posterior inference for acoustic response function

Under the assumption that the acoustic noise is Gaussian and its covariance is known it can be whitened and the likelihood function is therefore Gaussian. It follows that the posterior density of the acoustic Green's function over the symboling epoch is

$$p(\mathbf{h}|\mathbf{r}, \mathbf{b}) \propto N_{\mathbf{r}}(C_{\mathbf{b}} \underbrace{U_{\Delta,\tau}^{-1}\mathbf{h}}_{\mathbf{h}_{t,\tau}}, I) \times$$
$$\prod_{l,k} \left(\pi_\Delta N_{h_{l,k}}(0, \lambda_{l,k}^2) + (1 - \pi_\Delta) N_{h_{l,k}}(0, \epsilon_{l,k}^2) \right). \tag{17}$$

Assume that the symbols exhibit orthogonality over the delay, i.e. $C_{\mathbf{b}}$ satisfies $C_{\mathbf{b}}' C_{\mathbf{b}} = I$ recalling that the Fourier transform U is unitary we have

$$p(\mathbf{h}|\mathbf{r},\mathbf{b}) \propto N_{\mathbf{h}}(\check{\mathbf{h}}, I) \times \prod_{l,k} \pi_\Delta N_{h_{l,k}}(0, \lambda_{l,k}^2) + (1-\pi_\Delta) N_{h_{l,k}}\left(0, \epsilon_{l,k}^2\right)$$

and refactoring the product of Gaussian densities implies

$$p(\mathbf{h}|\mathbf{r},\mathbf{b}) \propto \prod_{l,k} (\pi_{\check{h}_{l,k}} N_{h_{l,k}}(\gamma(\lambda_{l,k})\check{h}_{l,k}, \gamma(\lambda_{l,k})) + (1-\pi_{\check{h}_{l,k}}) N_{h_{l,k}}(\gamma(\epsilon_{l,k})\check{h}_{l,k}, \gamma(\epsilon_{l,k}))) \quad (18)$$

where the least squares estimates are

$$\check{\mathbf{h}}_{\Delta,\tau} = U_{\Delta,\tau}\check{\mathbf{h}}_{t,\tau} \quad , \quad \check{\mathbf{h}}_{t,\tau} = C'_{\mathbf{b}}\mathbf{r}$$

and

$$\pi_{\check{h}_{l,k}} = \left(1 + \frac{1-\pi_\Delta}{\pi_\Delta}\frac{N_{\check{h}_{l,k}}(0, \epsilon_{l,k}^2 + 1)}{N_{\check{h}_{l,k}}(0, \lambda_{l,k}^2 + 1)}\right)^{-1}$$

$$\gamma(x) = \frac{x^2}{x^2+1} .$$

Since mixture Gaussian priors are conjugate for Gaussian likelihood functions the posterior density (18) is also a mixture Gaussian. The posterior mean is a weighted average of each model's average and since the posterior model probabilities π are also functions of the data the result, while akin to a classic Wiener filter, has an additional adaptable feature in the mixture weights. The result is a shrinkage operator of the raw delay-Doppler measurements $\check{\mathbf{h}}_{\Delta,\tau}$,

$$E[h_{l,k}|\mathbf{r},\mathbf{b},\hat{\epsilon},\hat{\lambda}] = \left(\pi_{\check{h}_{l,k}}\gamma(\lambda_{l,k}) + (1-\pi_{\check{h}_{l,k}})\gamma(\epsilon_{l,k})\right)\check{h}_{l,k}$$

which is written in compact form with S denoting the soft shrinkage rule

$$\hat{\mathbf{h}}_{\Delta,\tau} = S_{\check{\mathbf{h}}}(\check{\mathbf{h}}_{\Delta,\tau}). \quad (19)$$

This posterior expectation greatly attenuates smaller, noise-like coefficients while leaving the larger coefficients unchanged. The γ's are Wiener-like gains over each delay-Doppler element. The variance is

$$\begin{aligned} \hat{v}_{l,k} = var[h_{l,k}|\mathbf{r},\mathbf{b},\hat{\epsilon},\hat{\lambda}] &= \left(\pi_{\check{h}_{l,k}}\gamma(\lambda_{l,k}) + (1-\pi_{\check{h}_{l,k}})\gamma(\epsilon_{l,k})\right) \\ &+ \pi_{\check{h}_{l,k}}(1-\pi_{\check{h}_{l,k}})(\gamma(\lambda_{l,k}) - \gamma(\epsilon_{l,k}))^2 \times \check{h}_{l,k}^2 \end{aligned} \quad (20)$$

and can be understood as $\mathrm{var}[h_{l,k}] = E_{z_{l,k}}\mathrm{var}[h_{l,k}|z_{l,k}] + \mathrm{var}_{z_{l,k}} E[h_{l,k}|z_{l,k}]$. The parameters $\{\lambda_{l,k}, \epsilon_{l,k}, \pi_\Delta\}$ allow for adaptation of the model to the observations and they, like the gains, are estimated from the data, see for instance[9]. The Laplace approximation to the posterior distribution of the acoustic response function in the delay-time domain is therefore

$$p(\mathbf{h}_{t,\tau}|\mathbf{r},\mathbf{b},\hat{\epsilon},\hat{\lambda}) \approx N_{\mathbf{h}}(U_{\Delta,\tau}^{-1}\hat{\mathbf{h}}_{\Delta,\tau}, U_{\Delta,\tau}^{-1}\Upsilon U_{\Delta,\tau}^{-1}) \quad \Upsilon = \mathrm{Diag}(\hat{v}). \quad (21)$$

A computationally reasonable approximation to $E[\mathbf{h}|\mathbf{r}] = E_{\mathbf{b}}E[\mathbf{h}|\mathbf{r},\mathbf{b}]]$ is

$$E[\mathbf{h}|\mathbf{r},\mathbf{b}]] \approx U_\Delta^{-1} S_{E_{\mathbf{b}|\mathbf{r}}[\check{\mathbf{h}}]}(E_{\mathbf{b}|\mathbf{r}}[\check{\mathbf{h}}_{\Delta,\tau}]) \quad (22)$$

where

$$E_{\mathbf{b}|\mathbf{r}}[\check{\mathbf{h}}_{t,\tau}] = \sum \check{\mathbf{h}}_{t,\tau}(\mathbf{b})p(\mathbf{b}|\mathbf{r}) \ .$$

Figure 1 displays and comparse the least squares channel estimate and the posterior mean estimate based on the proposed mixture Gaussian model for an acoustic response function taken in St. Margaret's Bay. These are both for the same 2-ary spread spectrum signal set at -14 dB received SNR. The least square estimate is to the left and the MMSE posterior mean estimate based on the proposed mixture Gaussian model is to the right. Figure 2 shows a similar result for 4-ary signal epoch at a received SNR of -9 dB. In both figures 1 and 2 the power of the posterior mean to denoise dominant and faint arrivals as well as null the delay bands that are dominated by noise is apparent.

3 ESTIMATION OF AGGREGATE PATH DILATION

One of the critical advantage of accurate coherent estimates of the acoustic response function is that the bulk (aggregate, shared or common) dilation process associated with the acoustic arrival delay times can be estimated and factored out of the Green's function by "un-dilating" the received acoustic waveform. These path delay time processes are driven largely by source receiver motion in the case of mobile communicators but also by common ocean volume forces. For many underwater acoustic applications platform velocity is relatively minimal in the vertical direction as vehicles typically transit at a constant depth. For small acoustic angle spreads in shallow water, less than 15° range rate is a dominant factor in the shared delay time process. These arrival time variations for horizontally moving platforms are correlated having common time varying components that can be factored out to increase effective channel coherence. These facts account for the efficacy of phase tracking algorithms and the phase locked loop [15] for mobile commmunications and underwater acoustic communications[18] in particular. Here a subtly different approach is taken; the acoustic response function captures all delay-Doppler behavior over the signaling epoch up to the resolution of the symbol duration and the aggregate arrival time variations are then deduced from this estimate. The bulk path dilation estimate defines a natural (time-varying) sampling rate for the acoustic response that nearly "straightens out" or compenstates for the shared time variation of the acoustic paths. The remaining time variations of the acoustic arrivals constitute the natural coherence time of the ocean acoustic response function.

The Doppler bandwidth $1/2N_sW$ associated with the symbol interval determines the bandwidth of the final estimate and this is set by the processing gain and signaling bandwidth. Consider the two cases: 1) Time invariance dilation, that is, the shared component of the delay paths is a

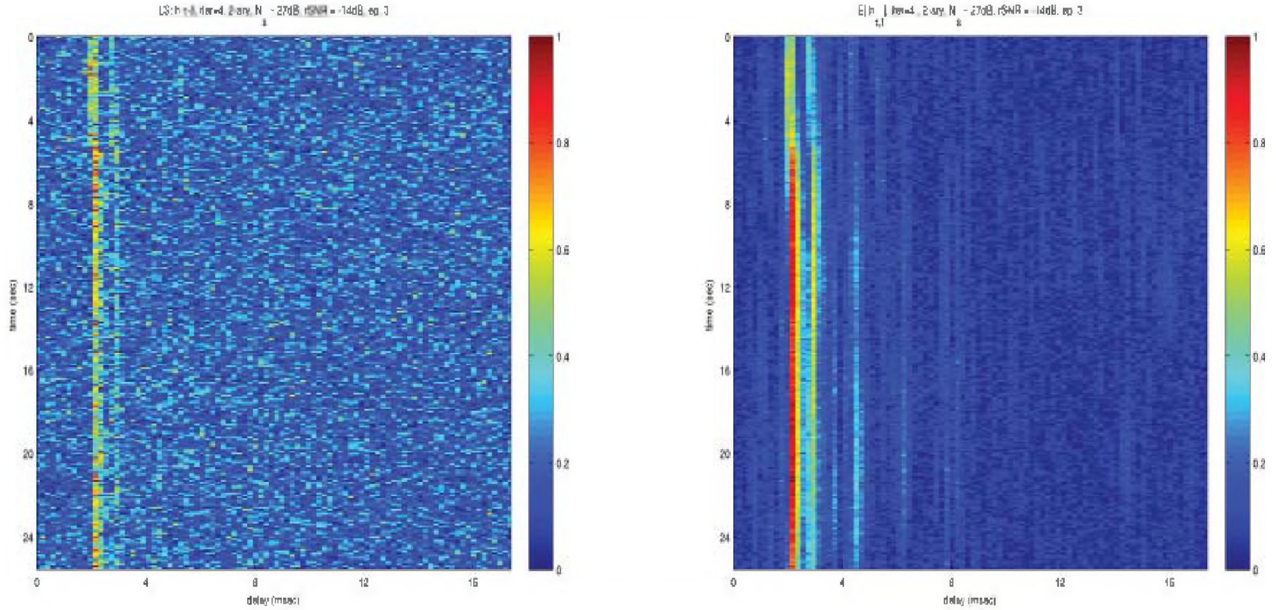

(a) (b)

Figure 1: Qualitative performance comparison of least squares channel estimate (left) with MMSE channel estimate based on Gaussian mixture model. Received SNR is -14 dB. Both are from the same 2-ary orthogonal spread spectrum data set.

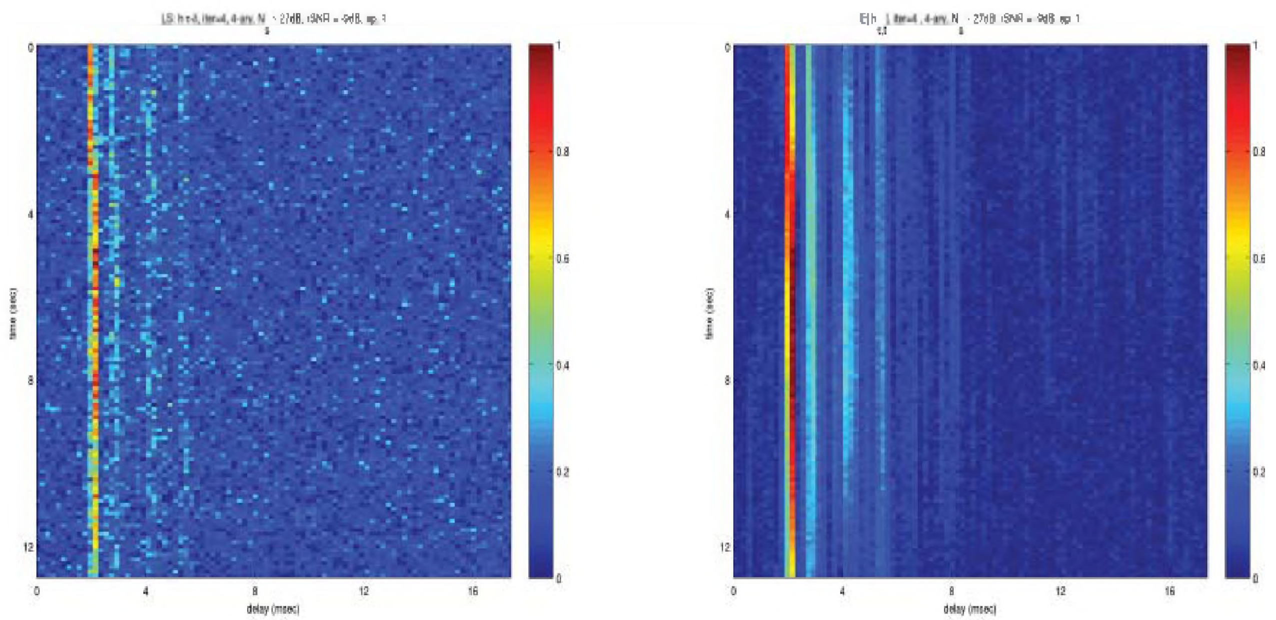

(a) (b)

Figure 2: Qualitative performance comparison of least squares channel estimate (left) with MMSE channel estimate based on Gaussian mixture model. Received SNR is -9 dB. Both are from the same 4-ary orthogonal spread spectrum data set.

simple linear function of time synonymous with a constant Doppler offset for all paths. 2) Time varying dilation. Allow for a common, shared temporal variation in the acoustic arrival times over the symboling interval. In the following subsections each of these is considered and suitable estimators are developed.

3.1 Time invariant path dilation rate

Factoring out a common linear delay drift, consider the model of the M_{path} dimensional arrival process as

$$\tau_m(t) = \delta_o \times t + \delta\tau_m(t) \ \ , \ m = \{1, \ldots M_{path}\} \tag{23}$$

where δ_o is a shared dilation rate among all of the paths. This factoring is obviously not unique and therefore we will seek to specify it in such a way that an appropriately weighted combination of the $\delta\tau_m(t)$ are minimized. To do this express the channel of Eq. (14) over Doppler frequency Δ, and channel frequency f, as

$$h_{\Delta,f} = \phi(f) \sum_m \int e^{-j2\pi(\Delta+(f+f_c)\delta_o)t} \times a_m(t, f+f_c) e^{-j2\pi(f+f_c)\delta\tau_m(t)} dt. \tag{24}$$

Let

$$\tilde{\psi}^o_{m,\Delta,f} = \phi(f) \int e^{-j2\pi\Delta t} a_m(t, f+f_c) \times e^{-j2\pi(f+f_c)\delta\tau_m(t)} dt \tag{25}$$

denote the m^{th} residual acoustic arrival response demodulated by frequency δ_o. Express the channel response, frequency shifted by δ_o, as

$$h_{\Delta-(f+f_c)\delta_o,f} = \sum_m \psi^o_{m,\Delta,f} \quad . \tag{26}$$

The Doppler spread for this particular acoustic response can be defined as

$$\int \Delta^2 |h_{\Delta-(f+f_c)\delta_o,f}|^2 d\Delta \quad .$$

Choose as an estimate of δ_o the value that minimize the total Doppler spread of the Doppler shifted version:

$$\hat{\delta_o} = \arg\min_{\delta_o} \int \Delta^2 |\hat{h}_{\Delta-(f+f_c)\delta_o,f}|^2 d\Delta df \quad . \tag{27}$$

This implies that the solution obeys

$$\int \Delta |\hat{h}_{\Delta-(f+f_c)\hat{\delta_o},f}|^2 d\Delta df = 0, \tag{28}$$

which can be interpreted as the expectation or the average over the Doppler spectral density $|\hat{h}_{\Delta-(f+f_c)\hat{\delta_o},f}|^2$. The Doppler offset for the given δ_o is proportional to the channel frequency $(f + f_c)$. The solution for a given f is

$$(f+f_c)\hat{\delta_o}(f) = \frac{\int \Delta |\hat{h}_{\Delta,f}|^2 d\Delta}{\int |\hat{h}_{\Delta,f}|^2 d\Delta}$$

and averaged over the entire bandwidth is

$$\hat{\delta_o} = \int \frac{\Delta}{(f+f_c)} \frac{|\hat{h}_{\Delta,f}|^2}{\int |\hat{h}_{\zeta,\xi}|^2 d\zeta d\xi} d\Delta df. \tag{29}$$

3.2 Time-varying path dilation rate

Consider now factoring out a common time-varying delay process from each of the path arrival times. Doing so leads to a model of the M_{path} arrival time processes as

$$\tau_m(t) = \tau_o(t) + \Delta\tau_m(t) \ \ , \ m = \{1, \ldots M_{path}\}. \tag{30}$$

As a function of $\tau_o(t)$ the acoustic response function Eq. (11) is

$$h_{t,\tau} = e^{-j\omega_c\tau_o(t)} \sum_m e^{-j\omega_c\Delta\tau_{m,t}} \times \tilde{\psi}_{m,t}(\tau - \tau_{m,t}) \tag{31}$$

and recalling that the conditional mean of the response function in delay-time is $\hat{\mathbf{h}}_{t,\tau}$ a computationally efficient estimation method for $\tau_o(t)$ is to consider the Laplace approximation to the density of $\mathbf{h}|\mathbf{r}$ and find its maximum with respect to $\tau_o(t)$. Define the bandwidth associated with the bulk dilation process as W_o and further let the bandlimited version of $\hat{h}_{t,\tau}$, the posterior mean estimate of the channel from data be denoted as

$$\hat{h}^o_{t,\tau} = \int_{W_o} \hat{h}_{\Delta,\tau} e^{j2\pi\Delta\times t} d\Delta. \tag{32}$$

Approximate the bulk dilation process with

$$\begin{aligned} \hat{\tau_o}(t) &= \arg\max_{\tau_o(t)} < \hat{h}_{t,\tau}, h_{t,\tau}(\tau_o(t)) > \\ &= \arg\max_{\tau_o(t)} Re\{\int \hat{h}_{t,\tau} \times h'_{t,\tau}(\tau_o(t)) d\tau\} \end{aligned} \tag{33}$$

leading to

$$\hat{\tau_o}(t) = \arg\max_{\tau_o(t)} \quad e^{+j\omega_c\tau_o(t)} \int |\hat{h}_{t,\tau}| e^{j\angle\hat{h}_{t,\tau}} \times \sum_m e^{+j\omega_c\Delta\tau_{m,t}} \tilde{\psi}'_{m,t}(\tau - \tau_{m,t}) d\tau. \tag{34}$$

To average out the $\tilde{\psi}'_{m,t}(\cdot)$ and $\Delta\tau_{m,t}$ assume that the remaining time varying phase variations $\{e^{+j\omega_c\Delta\tau_{m,t}}\}$ are negligibly small. This crude assumption allows us to approximate

$$\sum_m e^{+j\omega_c\Delta\tau_{m,t}} \tilde{\psi}'_{m,t}(\tau - \tau_{m,t}) = |\hat{h}_{t,\tau}| e^{j\angle h(0,\tau)}.$$

It follows that

$$\begin{aligned} \hat{\tau_o}(t) &= \arg\max_{\tau_o(t)} Re\{e^{+j\omega_c\tau_o(t)} \times \\ & \int |\hat{h}_{t,\tau}|^2 \times e^{j(\angle\hat{h}_{t,\tau} - \angle\hat{h}_{0,\tau})} d\tau\} \end{aligned} \tag{35}$$

so that a nearly maximum likelihood solution to $\tau_o(t)$ is

$$\hat{\tau_o}(t) = \omega_c^{-1} arg \left[\int |\hat{h}_{t,\tau}|^2 \times e^{j\angle\hat{h}_{t,\tau} - \angle\hat{h}_{0,\tau}} d\tau \right]. \tag{36}$$

This estimator weighs the phase rotation rate at each delay in proportion to it's energy so that the dominant arrivals dominate the estimate.

3.3 Inversion of the aggregate time dilation function

The proposed mixture Gaussian adaptive filtering scheme and the associated estimate of the bulk diation rate enable an increase in the effective channel coherence by unraveling the effect of the aggregate dilation, $\tau_o(t)$. This is accomplished by re-sampling the received data at a time-varying rate associated with the inverse of $u(t) = t - \tau_o(t)$. Recalling Eq. (10), note that

$$Hs(t) = \sum_n c_n^{\mathbf{b}} \times e^{-j\omega_c u(t)} \sum_m e^{-j\omega_c \Delta\tau_m(t)} \times \\ \tilde{\psi}_{m,t}(u(t) - \Delta\tau_{m,t} - n/W) \\ u(t) = t - \tau_o(t).$$

Since the dilation rates are much smaller than the acoustic propagation speed the function $u(t)$ is a monotonically increasing function with a unique inverse $t = \nu \circ u \circ t$ and therefore Hs can be expressed as a function of u the natural time variable for the acoustic observations,

$$Hs(v \circ u) = \sum_n c_n^{\mathbf{b}} \times e^{-j\omega_c u} \sum_m e^{-j\omega_c \Delta\tau_m(\nu \circ u)} \times \\ \tilde{\psi}_{m,\nu\circ u}(u - \Delta\tau_m(\nu \circ u) - n/W). \quad (37)$$

This is done to specify the inverse of the time dilation operator u. To do this, note that incremental differences in the two sampling grids are: $t - u = \tau_o(t)$, exactly the time varying dilation rate. Now approximate $\tau_o(t)$ as a function of u by a first order Taylor expansion $\tau_o(t) \approx \tau_o(u) + \partial_u \tau_o(u)(t - u)$ so that

$$t - u \approx \tau_o(u) + \partial_u \tau_o(u)(t - u) \\ \tau_o(u) = (t - u)(1 - \partial_u \tau_o(u)) \\ t = u + \frac{\tau_o(u)}{1 - \partial_u \tau_o(u)},$$

and it follows that

$$\nu \circ u(t) = t \quad , \quad \nu(x) = x + \frac{\tau_o(x)}{1 - \partial_x \tau_o(x)} \quad . \quad (38)$$

The estimate of the resampling operator ν is derived from the estimated bulk dilation rate $\tau_o(t)$ via a one to one map. The estimation process conditioned on the previous estimate of the symbol set can be summarized as follows:

$$\underset{E[\cdot|r,b]}{\hat{\mathbf{h}}} \Longrightarrow \underset{\approx \arg\max p[\cdot|r,b]}{\hat{\tau}_o(t)} \underset{one-to-one}{\Longrightarrow} \hat{\nu} \quad \hat{\nu} \circ \hat{u} = t \quad (39)$$

3.4 Effect of resampling operator on acoustic response function

Considering again the model of the received pressure imparted from the information bearing source (37) on the receiver element as

$$Hs \circ \nu(u) = e^{-j\omega_c u} \sum_n c_n^{\mathbf{b}} \sum_m e^{-j\omega_c \Delta\tau_m \circ \nu(u)} \times \\ \tilde{\psi}_{m,\circ\nu(u)}(u - \Delta\tau_m \circ \nu(u) - n/W)$$

the baseband demodulated and resampled acoustic response function can be identified as

$$h^\nu(u,\tau) = \sum_m e^{-j\omega_c \Delta\tau_m^\nu(u)} \times \tilde{\psi}_{m,u}^\nu(\tau - \Delta\tau_m^\nu(u)) \quad (40) \\ \Delta\tau_m^\nu(u) = \Delta\tau_m \circ \nu(u) \quad , \quad \tilde{\psi}_m^\nu(\tau) = \tilde{\psi}_{m,\circ\nu(u)}(\tau).$$

Since Eq. (40) is of the same form as (10) the resampling operator can be decomposed into a set of composite resampling operators consistent with an iterative joint estimation based receiver. If the function $\nu(t)$ is well estimated from the data the bandwidth of the residual channel response parameterized by $\psi_{m,u}, \Delta\tau_m^\nu$ will on average be less than that of the original sampled processes.

To illustrate the value of the proposed scheme as a means to focus coherent acoustic energy dispersed in Doppler bandwidth by source-receiver motion consider the application of the proposed dilation compensation method. Figure 3 presents an example of an acoustic Green's function in Doppler[Hz] and channel frequency[kHz] comparing time-invariant dilation and time varying dilation. In both cases the results are taken from a joint symbol and channel estimation procedure associated with an acoustic communications signal. The estimator on the left is that of one iteration after initial channel and symbol estimates. The estimator to the right is that of the third iteration following time varying Doppler compensation. The significant focusing and narrowing of the Doppler bandwidth of the response function is observed.

4 AN M-ARY ORTHOGONAL SIGNALING FOR UNDERWATER ACOUSTIC COMMUNICATIONS

The signaling scheme that is used to test these proposed adaptive filtering schemes is similar to that of the M-ary Walsh/m-sequence signaling tested by Iltis [11]. Performance bounds have been derived for M-ary orthogonal spread spectrum signaling through fading channels for the case of independent channel gains [17][1][6][7][14] and specific algorithms for diversity combining of M-ary orthogonal signals have been explored [19]. In this present study it is assumed that the symbol sets have good orthogonal properties over the multipath spread of the acoustic channel. The essential feature of such an M-ary signal set is that the symbol sequences $\mathbf{c}_m$, $m = 1, ...M$, obey

$$C_k' C_l = I \times \delta_{k-l} + E_{k,l} \quad (41)$$

where C_m is the convolution operator associated with the code word $\mathbf{c}_m$. The matrix E has all coefficients less than $1/N_s$ where N_s is the sequence length. The receiver estimates the bit stream sent by

$$\begin{aligned} \hat{\mathbf{h}}^i &= E_{h|b=\hat{b}}[\mathbf{h}|\mathbf{r}, \mathbf{b} = \hat{\mathbf{b}}^{i-1}, \tau_o = \hat{\tau_o}^{i-1}] \\ \hat{\mathbf{b}}^i &= \arg\max_{\mathbf{b}} p(\mathbf{b}|\mathbf{r}, \mathbf{h} = \hat{\mathbf{h}}^i, \tau_o = \hat{\tau_o}^i) \quad (42) \\ \hat{\tau_o}^i &= \arg\max_{\tau_o} p(\mathbf{h}_{\tau_o}|\mathbf{r}, \mathbf{b} = \hat{\mathbf{b}}^{i-1}). \end{aligned}$$

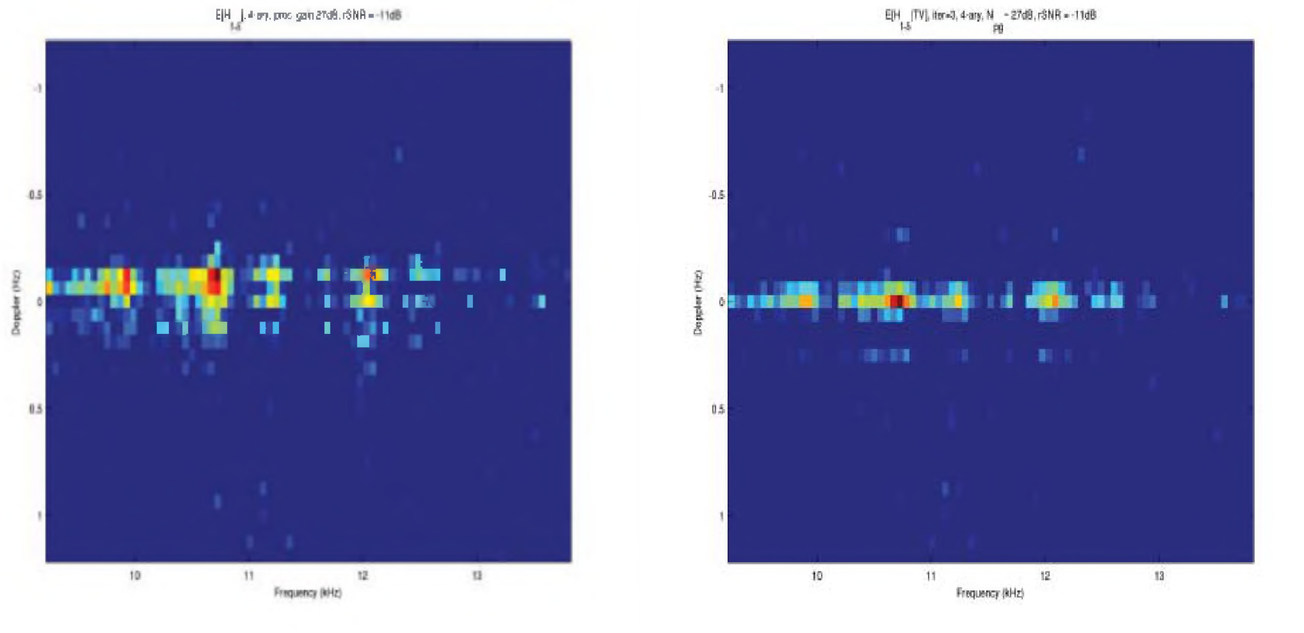

(a) (b)

Figure 3: Display of acoustic response functions demonstrating the focusing of energy in Doppler that attends time varying dilation estimation and compensation (40). Channel estimates were taken from the same 4-ary orthogonal data sets. Left, with only time invariant Doppler compensation. Right, with time-varying Doppler compensation.

Here, as previously, $\mathbf{h}$ represents the double spread channel function, $\mathbf{b}$ represents the sent bit stream of interest and τ_o represents the aggregate time varying dilation rate. Iterative receiver structures can now be constructed from any of the various conditional estimators of channel and dilation rate coupled to symbol decisions conditioned on those estimates. In this section a few such receivers that provide a good compromise between accuracy and computational cost are discussed. Coherent and non-coherent symbol decisions are considered but only of the hard decision type.

4.1 Symbol decision rules

In this channel estimation based scheme symbol decisions are made conditioned on the data $\mathbf{r}$ and the channel parameter estimates which of course are functions of the data. For simplicity we ignore the variance of the channel estimates in the decision process. The likelihood function for each symbol is of the form

$$\mathbf{r}_t|\mathbf{h}_t, b_t \sim N_{\mathbf{r}}(C_{b_t}\mathbf{h}_t, I) \qquad b_t \in \{1, 2 \dots M\}$$

where b_t specifies the sent codeword at the t^{th} symboling frame determining the $N_s + L - 1 \times L$ convolution operator C_{b_t}.

4.2 Coherent soft and hard decisions

With equally probable and equal energy symbols the probability of $b = m \in$ and ignoring the variance of the channel function estimation errors approximate as $P(b = m|\mathbf{r}, \mathbf{h} = \hat{\mathbf{h}}) = p(\mathbf{r}|b = m, \mathbf{h}) / \sum_{m'} p(\mathbf{r}|b = m', \mathbf{h} = \hat{\mathbf{h}})$. The results is

$$P(b_t = m|\mathbf{r}, \mathbf{h}) \approx \frac{e^{2Re[\hat{\mathbf{h}}' C'_m \mathbf{r}_t]}}{\sum_l e^{2Re[\hat{\mathbf{h}}' C'_l \mathbf{r}_t]}} \tag{43}$$

and approximate ML decisions conditioned on the channel iteration estimate are

$$\hat{b}_t \approx \underset{m}{\arg\max} \quad Re[\tilde{\mathbf{h}}'_t C'_m \mathbf{r}_t] \quad (\mathrm{WPC-C}). \tag{44}$$

We denote this symbol decision rule as weighted path combining with coherent decisions (WPC-C).

4.3 Noncoherent soft and hard decisions

Likewise non-coherent symbol estimates and decisions are based on $|\hat{\mathbf{h}}' C'_m \mathbf{r}_t|^2$. Assume perfect orthogonality of the symbol code words over the L lag delay band $C_m C_{m'} = I_L \delta_{m-m'}$ and for simplicity in what follows define $\tilde{\mathbf{h}} = \mathbf{h}/|\mathbf{h}|^2$ and noting that the M statistically independent $\tilde{\mathbf{h}}' C'_k \mathbf{r}_t$ complex scalar variables are Gaussian distributed

$$\begin{aligned} \tilde{\mathbf{h}}'_t C'_m \mathbf{r}_t | b_t = m &\sim N_x(|\mathbf{h}|_2, 1); \\ \tilde{\mathbf{h}}'_t C'_m \mathbf{r}_t | b_t \neq m &\sim N_x(0, 1) \end{aligned}$$

so that

$$\begin{aligned} x_m^2 = |\tilde{\mathbf{h}}' C'_m \mathbf{r}_t|^2 &\sim \chi_2^2(|\mathbf{h}|_2^2) \;, \\ x_{k|m}^2 = |\tilde{\mathbf{h}}' C'_k \mathbf{r}_t|^2 &\sim \chi_2^2 \end{aligned} \tag{45}$$

Table 1: MPC receiver

MPC	
Parameter	Estimator
bulk path dilation: $\Delta\tau^o$	N/A
symbol decision:	Eq. (48)
channel estimate:	N/A

where $\chi_2^2(\lambda^2)$ represents a non-central chi-square random variable [13] with non-centrality parameter λ^2 and $\chi_2^2 = \chi_2^2(0)$ is the standard central chi-square random variable. Let $p_{\chi_2^2(\lambda)}(x)$ denote the density function of a non-central chi-square random variable with non-centrality parameter λ. It follows that symbol probabilities can be approximated by conditioning on the estimated channel response. It follows that $P(b_t = m|x_1^2, \ldots, x_M^2), \mathbf{h} = \hat{\mathbf{h}}) = p(\mathbf{r}|b = m, \mathbf{h})/\sum_{m'} p(\mathbf{r}|b = m', \mathbf{h} = \tilde{\mathbf{h}})$ and therefore

$$P(b_t = m|\mathbf{r}, \mathbf{h}) \approx \frac{p_{\chi_2^2(|\hat{\mathbf{h}}|^2)}(|\tilde{\mathbf{h}}' C_m' \mathbf{r}_t|^2)}{\sum_{k \in \mathcal{M}} p_{\chi_2^2(|\hat{\mathbf{h}}|^2)}(|\tilde{\mathbf{h}}' C_k' \mathbf{r}_t|^2)} \quad . \tag{46}$$

Hard decisions are simply

$$\hat{b}_t = \arg\max_m \ |\hat{\mathbf{h}}_t' C_m' \mathbf{r}_t|^2 \ (\mathrm{WPC-NC}). \tag{47}$$

Denote this symbol decision rule as weighted path combining with non-coherent decision (WPC-NC). These decision schemes will be compared to a maximal path combining (MPC) scheme that does not require channel estimation. While intuitively simple, the detail is worth stating. Let $\mathbf{x}^{(k)}$ be the kth ranked order statistic of $\mathbf{x}$ then choose the greatest L^* ranked outputs and sum. This can be expressed succinctly as

$$\hat{b}_t = \arg\max_m \sum_{(k)=1}^{L^*} \mathbf{x}_m^{(k)} \ , \ \mathbf{x} = \check{\mathbf{h}}_m^2 \ , \ \ (\mathrm{MPC}). \tag{48}$$

$$\check{\mathbf{h}}_m = C_m' \mathbf{r}_t.$$

Table states the computationally fast maximal path combining (MPC) receiver where the decisions are based not on estimated $\mathbf{h}$ but on simply the L^* maximum coefficients of $\check{h}$, the matched filter outputs. Table 1 summarizes the maximal path combining receiver and Table 2 summarizes the channel estimation and dilation compensation based iterative receiver structures.

Figure 4 displays the performance of the proposed algorithm in terms of bit error rate as a function of iteration. Iteration one and iteration three are shown. Iteration one does not have time varying dilation estimation and iteration three does. The improvement by iteration three is approximately 2 dB, a significant performance gain. The results show that for 2-ary signaling at -12 dB received SNR the bit error rate is below 10^{-4}. For 4-ary signaling at -9 dB received SNR the bit error rate is below 10^{-6}. In each case the spreading gain is approximately 27 dB.

5 RESULTS.

The proposed adaptive filtering scheme was implemented in a channel estimation based communication receiver enabling coherent multipath combining of M-ary orthogonal signals and allowing the comparison with conventional schemes. The proposed iterative receiver structures were tested on signals of the Unet-08 M-ary orthogonal spread spectrum experiment of June 2008 taken in St. Margaret's Bay. Probability of bit error over a range of SNRs were computed by Monte-Carlo averaging of the receiver's error rate statistics. Presented here are comparisons of coherent channel estimate based results with maximal path combining, as well as coherent and noncoherent symbol decisions. All results are for single element reception. Array gain is not employed. The receivers tested are listed and described in Table 2. Rough synchronization and Doppler estimation are derived from short (1 symbol duration) broad band synchronization signals that initializes the algorithm. For all cases tested the received signal to noise ratio (rSNR) is measured as the in-band signal power average to the whitened noise power average over the entire signaling packet. Throughput rates for these schemes are as follows: 2-ary corresponds to 10 bps. 4-ary corresponds to 20 bps. Each communication packet employs 27 dB of processing gain, $N_s = 512$. Signal bandwidth is roughly 5.12 kHz corresponding to one symbol every 1/10 of a second. Higher throughput rates can be achieved by employing larger bandwidths, reduced procssing gain or larger alphabet sizes.

The performance of M-ary orthogonal signaling through a single element AWGN channel with coherent and noncoherent decisions is displayed on all figures for reference as a lower bound on error rate performance. Figure 4 displays the performance as a function of receiver iteration for 2-ary and 4-ary for 3 different channel epochs. The probability of error for two of the signaling epochs for 2-ary and 4-ary are shown in each panel. It is observed that refinement of the channel estimate leads to improved decisions. For the case of 2-ary we see roughly a .5 dB to 1.5 dB improvement from the first to the third iteration. Further iterations improve only slightly. For 4-ary we see a more significant 3 dB to 4 dB improvement from the first to the third iteration.

Consider a comparison of the proposed method with simple maximal path combining (MPC). Shown in figure 5, it is observed that coherent multipath combining outperforms MPC by greater than 2 dB regardless of the M, alphabet size. This is attributed to accurate channel estimation allowing the weighing of lower power coherent paths and the rejection of spurious noisey paths. By down weighting the acoustic inter-arrival times significant performance gains are observed. It should be mentioned that MPC using more than the $L = 8$ maximal delay lag coefficients does not lead to improved results. If L is chosen too large significant degradation in performance results as noise power is added to the decision statistic. Since MPC requires a prior information regarding the number of paths to combine it is clear that the channel estimation based schemes proposed here have an additional advantage of adaptability to channel conditions.

Table 2: Iterative receiver algorithms for M-ary orthogonal spread spectrum signaling

Receiver 1		
WPC w/ non-coh. decisions without symbol-aided timing estimation		
Parameter	Initialization	Iterative estimator
symbol decision: $\mathbf{b}^i$	$p(\mathbf{b}^0) = M^{-K}$ or (MPC)	Eq. (47)
acoustic response: $\mathbf{h}^i$	Eq. (22)	Eq. (19)
resampling operator: ν	N/A	N/A
two iterations total		
Receiver 2		
WPC-non-coh. decisions with symbol-aided time-invariant timing estimation		
Parameter	Initialization	Iterative estimator
symbol decision $\mathbf{b}^i$	$p(\mathbf{b}^0) = M^{-K}$ or (MPC)	Eq. (47)
acoustic response: $\mathbf{h}^i$	Eq. (22)	Eq. (19)
bulk path dilation: $\Delta\tau^i$	Eq. (29)	Eq. (29)
resampling operator: ν	N/A	N/A
three symbol decision iterations total		
Receiver 3		
WPC w/ coh. decisions with symbol-aided time-varying timing estimation		
Parameter	Initialization	Iterative estimator
symbol decision: $\mathbf{b}^i$	$p(\mathbf{b}^0) = M^{-K}$ or (MPC)	Eq. (44)
acoustic response: $\mathbf{h}^i$	Eq. (22)	Eq. (19)
bulk path dilation: $\tau^i(t)$	Eq. (29)	Eq. (36)
resampling operator: ν	N/A	Eq. (38)
three symbol decision iterations total		

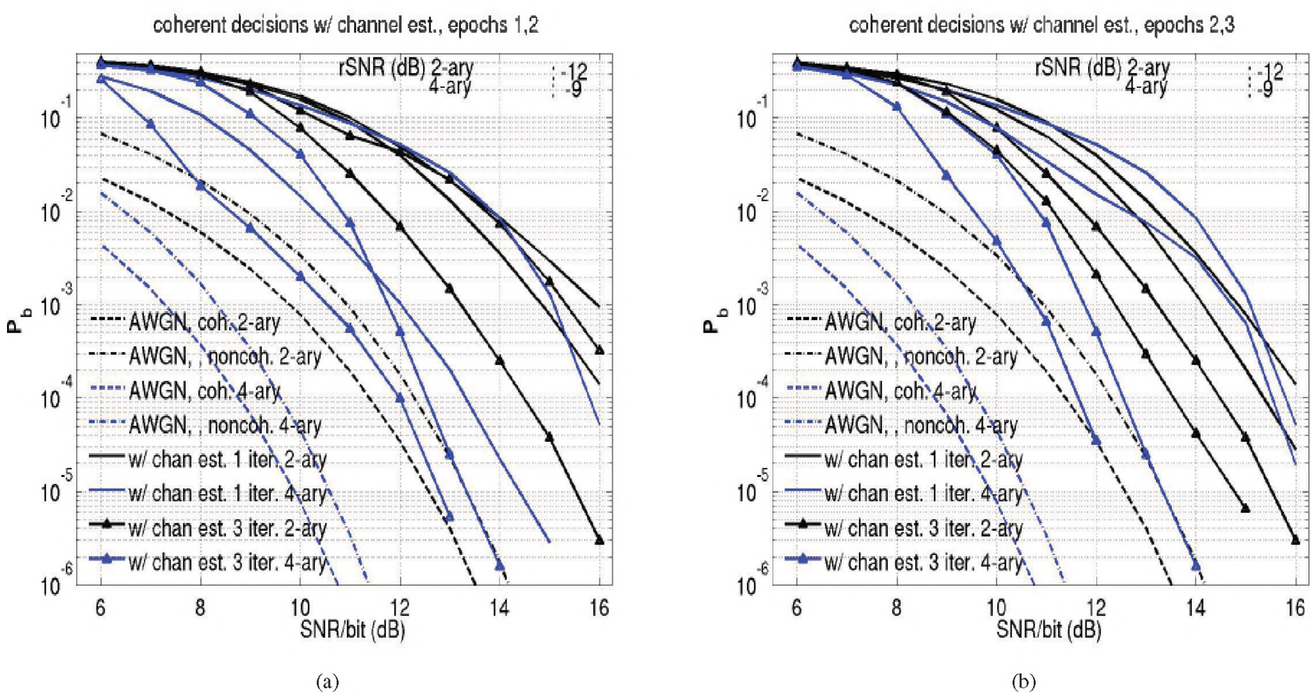

Figure 4: Performance of coherent multipath combining for M-ary orthogonal signaling with proposed adaptive filtering scheme as a function of iteration. Results are shown for signaling epochs 1 and 2 in the lefthand (a) graph and for epochs 2 and 3 on the righthand (b) graph. Performance bound for AWGN channels is shown as a dashed line.

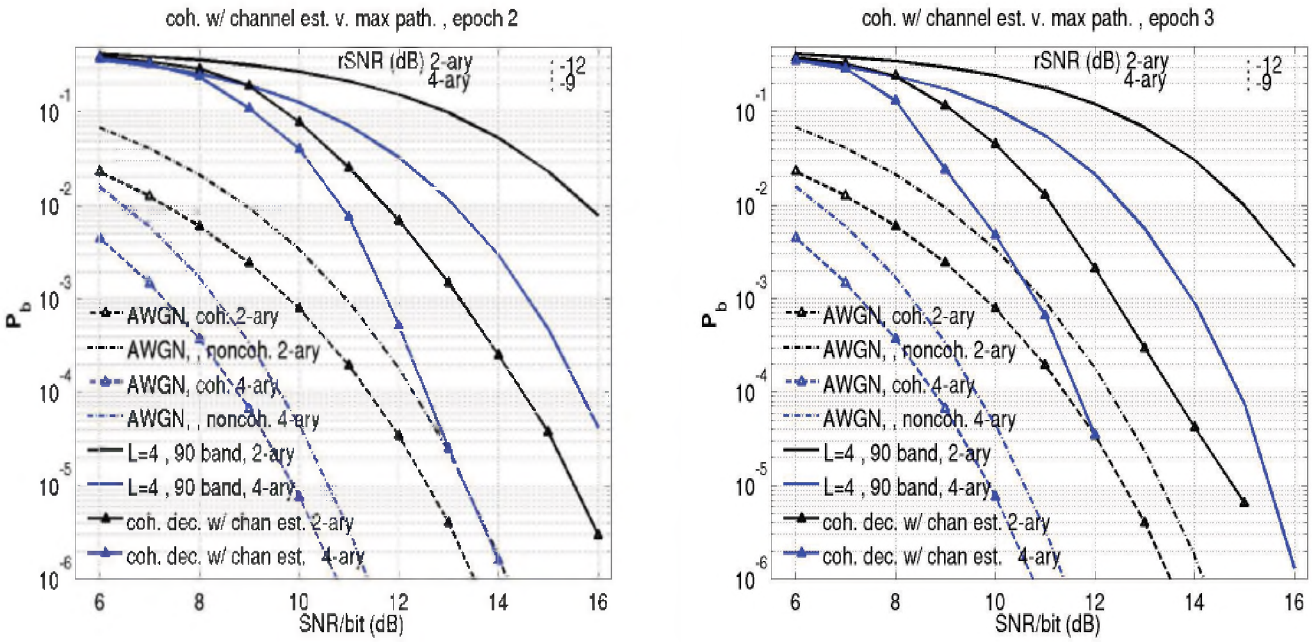

(a) (b)

Figure 5: Comparison of coherent combining of multipaths with channel estimation with that of maximal 4 paths combining (MPC) over a delay band of $W \times \tau_{max} = 90$. Improvement of 4 dB for 2-ary and 3 dB for 4-ary is apparent for all signaling epochs. AWGN bounds are shown as dashed lines.

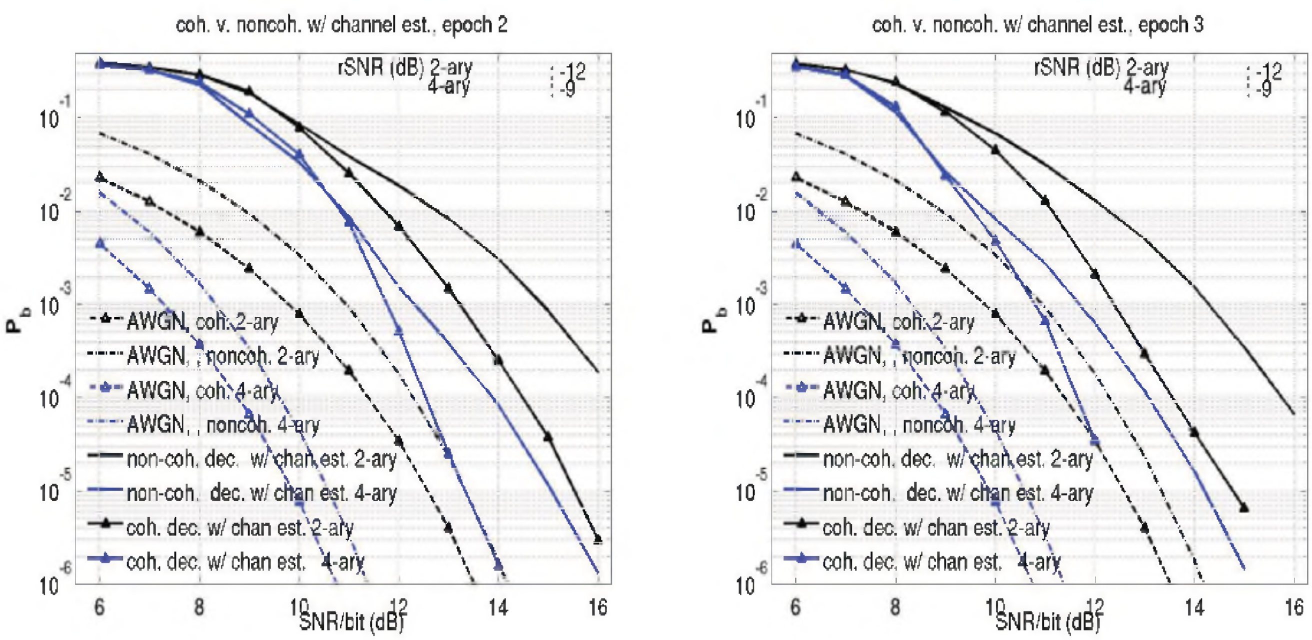

(a) (b)

Figure 6: Comparison of coherent decisions with channel estimation based coherent multipath combining with that non-coherent decisions. Improvements of up to 2 dB is observed for all signaling epochs for both 2-ary and 4-ary signaling is observed. AWGN bounds are shown as dashed lines.

It is worth comparing coherent decisions with non-coherent decisions. See Table 2 for the explicit computations with each. Figure 6 displays the performance of coherent channel estimation and multipath combining with coherent decisions against similar channel estimation with non-coherent decision. The receiver with Doppler compensation and coherent decisions outperforms that of non-coherent decisions over both signaling epochs and across signal to noise ratios. For 2-ary signaling a near 2 dB increase in performance is observed. For 4-ary the improvement with coherent decisions is also roughly 2 dB. It is observed that for 4-ary signaling an error rate of less than 10^{-4} is observed at -8 dB rSNR.

6 SUMMARY, CONCLUSIONS AND FUTURE WORK.

Mixture model based adaptive filtering schemes can incorporate all of the data in a signaling epoch to make accurate inferences regarding the acoustic response function at each symbol within the signaling epoch. These estimators enable iterative channel estimation based receiver algorithms for M-ary orthogonal communications in shallow water acoustic environments that can operatate at low SNR. Channel estimation is based on a Gaussian mixture model over Doppler and channel frequency that provides flexibility in the regularization of sparse acoustic channel estimates. The resulting estimator leaves acoustic arrivals that exhibit concentration of energy in Doppler unattenuated while greatly attenuating background noise and the incoherent highly dispersed low energy arrivals. This channel estimate forms the basis for time-varying aggregate path dilation estimation and resampling that effectively increases channel coherence to the natural coherence of the ocean media. Since signaling epochs can be quite long in duration reliable aggregate path dilation estimates require all of the data within a packet in order to operate efficiently at low SNR.

This scheme has been tested with a number of receiver implementations employing both coherent and non-coherent symbol decisions with the proposed channel estimation scheme. These novel channel estimation based weighted path combining schemes are compared to simple maximal path combining. The proposed receivers demonstrate between 3 and 4 dB of improvement over maximal path combining at received SNRs corresponding to a probability of error $< 10^{-5}$. For received SNRs of under -8 dB a probability of error of less than 10^{-4} for single element reception has been observed in the downward refracting environment of St. Margaret's Bay NS with a drifting source.

The schemes are well suited for low rate, low SNR underwater acoustic communications. They can be adapted to multi-user communications and MIMO applications. Future work will focus on modeling the dependence between delay-Doppler indicator variables $z_{k,l}$ for improved channel estimation and the extension of this mixture Gaussian model to beam angle for computationally fast beamforming for receiver arrays.

Acknowledgments

This work is supported by both the Office of Naval Research and by the Naval Innovative Science and Engineering Program. Thanks to Garry Heard of DRDC-Atlantic, for serving as Chief Scientist of the Unet08 experiments. Thanks to Dale Green of Teledyne Benthos for executing the Unet08 M-ary orthogonal acoustic experiments on the 4^{th} generation Teledyne Benthos modem.

REFERENCES

[1] V. Aalo, O. Ugweje, R. Sudhakar, "Performance analysis Analysis of DS/CDMA systems with noncoherent M-ary orthogonal modulation in Nakagami fading" *IEEE Trans. on Vehicular Technologies, Vol. 47, June 1999, pp 111-117.*

[2] P.J. Brockwell, R.A. Davis "Time Series: Theory and Methods, Second Edition", *Springer-Verlag*, ISBN 0-387-97429-6(USA), Springer Verlag, New York NY, 1991.

[3] Teledyne-Benthos, "Product Catalog 2010, Wireless Subsea Communications" *http://www.benthos.com/pdf/*

[4] P.J. Crepeau, "Asymptotic performance of M-ary orthogonal modulation in generalized fading channels" *IEEE Trans. Commun., Vol 36, No 11, November 1988, pp 1246-1249...*

[5] P. Dahl, et al., "Underwater Ambient Noise" *Acoustics Today*, Vol 3 Issue 1 pp 23-33. January 2007.

[6] A. Dekorsy, K.D. Kammeyer M-ary Orthogonal Modulation for Multi-Carrier Spread-Spectrum Uplink Transmission Proceedings of IEEE International Conference on Communications (ICC), Vol. 2 (June 1998), pp. 1004-1008.

[7] A. Dekorsy, S. Fischer, K. Kammeyer, Maximum likelihood decoding of M-ary orthogonal modulated signals for multi-carrier spread-spectrum systems Personal, Indoor and Mobile Radio Communications, 1998. The Ninth IEEE International Symposium on Boston MA, 8-11 Sep 1998, page(s): 538 - 543 vol.2, ISBN: 0-7803-4872-9 INSPEC Accession Number: 6275687, Digital Object Identifier: 10.1109/PIMRC.1998.734261

[8] N.R. Farnoud, M. Kolios and S. Krishnan, "Ultrasound Backscatter Signal Characterization and Classification Using Autoregressive Modeling and Machine Learning Algorithms", IEEE Conference Proceedings on Engineering in Medicine and Biology Society, vol. 3, pp. 2861 - 2864, Sep 17-21, 2003.

[9] P.J. Gendron, "An Empirical Bayes estimator for in-scale adaptive filtering" *IEEE Transactions on Signal Processing,* Vol. 56, No. 5, pp 1670-1683, May 2005.

[10] S. Haykin, "Adaptive Filter Theory", Prentice Hall Information and System Sciences Series, New Jersey, 2002.

[11] R. J. Iltis, "A Sparse Kalman Filter with Applicaiton to Acoustic Communications Channel Estimation" *IEEE/MTS OCEANS 2006*, ISBN 1-4244-0114-3, 18-21 September 2006.

[12] F.B. Jensen, W.A. Kuperman, M.B. Porter, H.Schmidt "Computational Ocean Acoustics", *AIP Press, AIP Series in Modern Acoustics and Signal Processing* ISBN 1-56396-209-8

[13] N.L. Johnson, S. Kotz, "Distributions in Statistics: Continuous univariate distributions-2," *John Wiley & Sons, Wiley Series in Probability and Mathematical Statistics, 1970.* ISBN 0-471-44627-0.

[14] I.D. Panagiotis, F-N. Pavlidou, DS/CDMA M-ary orthogonal signaling in shadowed Rayleigh channel for mobile communications, Wireless Networks, Vol. 2, pp 343-357.

[15] J. Proakis "Digital Communications", *McGraw-Hill, Inc.*, 1221 Avenue of the Americas, New York, NY 10020, 2000.

[16] M. de Oliveira Rosa, J.C. Pereira, M. Grellet, "Adaptive Estimation of Residue Signal for Vocal Pathology Diagnosis" *IEEE Trans. on Biomedical Engineering, Vol. 47, No. 1. January 2000, pp 96-104.*

[17] M.K. Simon, M.S. Alouini, "Bit error probability of noncoherent M-ary orthogonal modulation over generalized fading channels." *Int. J. Commun. and Networks, Vol 1, No 2. February 1998, pp 20-29.*

[18] M. Stojanovic, "Multichannel detection for wideband underwater acoustic CDMA communications" *Journal of Oceanic Engineering, 2006, Vol 31 No. 3 pp 685-695.*.

[19] J.S. Thompson, P.M. Grant, B. Mulgrew, "Algorithms for coherent diversity combining of M-ary orthogonal signals" *IEEE Journal on Selected Areas in Communications,* Vol 17, Issue 11, November 1999, pp 1886-1899.

[20] R. J. Urick, "Principles of Underwater Sound 3rd Edition" *Peninsual Publisher, 1996*. ISBN-13: 978-0932146625.

ICSV19
PRESS RELEASE

The 19th International Congress on Sound and Vibration (ICSV19), sponsored by the International Institute of Acoustics and Vibration (IIAV) and Vilnius University, will be held from 8 - 12 July 2012 at Vilnius University in Vilnius, Lithuania. Vilnius is the historical capital of Lithuania and dates back to the 14th century and has since been awarded the status of World Cultural Heritage by UNESCO. Vilnius University is one of the oldest universities in Eastern Europe and the friendly atmosphere of the modern city will mesmerize you and leave you with unforgettable memories.

Theoretical and experimental research papers in the fields of acoustics, noise, and vibration are invited for presentation. Participants are welcome to submit abstracts and companies are invited to take part in the ICSV19 exhibition and sponsorship. For more information, please visit < http://www.icsv19.org >.

For further details, please contact Malcolm J. Crocker at, crockmj@auburn.edu >.